

Chapter 4 Laminar Boundary Layers

4. Additional Topics

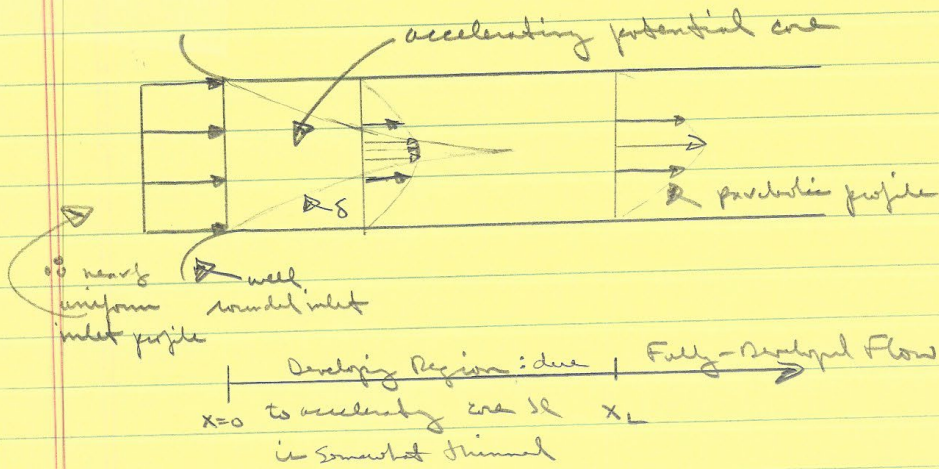
- a. Inlet Duct Flow
- b. Rotationally Symmetrical Boundary Layers
- c. Axisymmetric Boundary Layers
- d. 3D Boundary Layers
- e. Asymptotic Expansions
- f. Unsteady Boundary Layers

Choi, J.-E., Sreedhar, M., and Stern, F., "Stokes Layers in Horizontal-Wave Outer Flows," ASME J. Fluids Eng., Vol. 118, September 1996, pp. 537 – 545.

Paterson, E.G. and Stern, F., "Computation of Unsteady Viscous Marine-Propulsor Blade Flows - Part 1: Validation and Analysis," ASME J. Fluids Eng., Vol. 119, March 1997, pp. 145 – 154.

Paterson, E.G. and Stern, F., "Computation of Unsteady Viscous Marine-Propulsor Blade Flows - Part 2: Parametric Study," ASME J. Fluids Eng., Vol. 121, March 1999, pp. 139 – 147.

Inlet Duct Flow



2d theory can predict: x_L , excess Δp over Poiseuille law, and shape of the developing profiles

$$\bar{u} = \text{ave vel} = Q/A$$

$$u_p = 2\bar{u}(1 - v^2/a^2)$$

excess Δp follows from cv analysis

$$(p_0 - p_x) \pi a^2 = \tau_p 2\pi a x + \int_0^x (\tau - \tau_p) 2\pi a dx + \rho \int_0^x (u - \bar{u}) 2\pi v dx$$

$$2(p_0 - p_x) / \rho \bar{u}^2 = \lambda x / D + K \quad K = 2/3 + \int_0^{x/a} \frac{4(\tau - \tau_p)}{\rho \bar{u}^2} \frac{dy}{a}$$

contribution from acceleration of profile

$D = 2a$ pipe

$D = h$ channel

$$\lambda = \frac{8\tau_p}{\rho \bar{u}^2} = 64 / Re_D$$

$$\lambda = 96 / Re_h$$

Poiseuille friction coefficient

$$K = K(x, Re_D, \text{duct shape (pipe or channel)})$$

$$\sim 1.31 \text{ (pipe)} \cdot 0.67 \text{ (channel)}$$

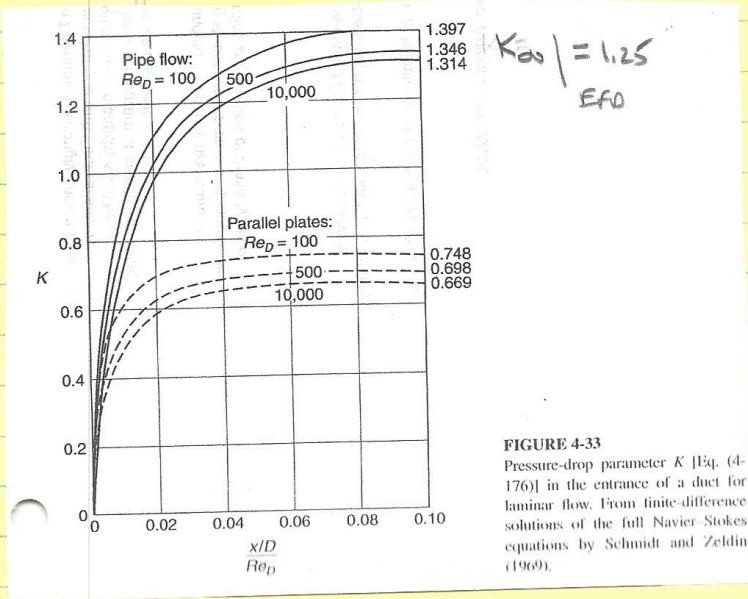


TABLE 4-7
Constants to be used in Eq. (4-177)

b/a	$C_{f,Re}$	K_{∞}	c
Pipe or Concentric Annulus			
0.0	16.00	1.25	0.000212
0.05	21.57	0.830	0.000050
0.10	22.34	0.784	0.000043
0.50	23.81	0.688	0.000032
0.75	23.97	0.678	0.000030
1.00	24.00	0.674	0.000029
Rectangular Duct			
1.00	14.23	1.43	0.00029
0.50	15.55	1.28	0.00021
0.30	19.07	0.931	0.000076
0.00	24.00	0.674	0.000029
Equilateral Triangle			
13.33	1.69		0.00053

FIGURE 4-33 Pressure-drop parameter K [Eq. (4-176)] in the entrance of a duct for laminar flow. From finite-difference solutions of the full Navier-Stokes equations by Schmidt and Zeldin (1969).

can also be written $\frac{2(p_0 - p_x)}{c \pi^2} = C_{f,app} 4x/D$

apparent friction $C_{f,app} Re = \frac{3.44}{\sqrt{s}} + \frac{C_{f,Re} + K_{\infty}/4s - 3.44/\sqrt{s}}{1 + c/s^2} \quad s = \frac{x/D}{Re}$

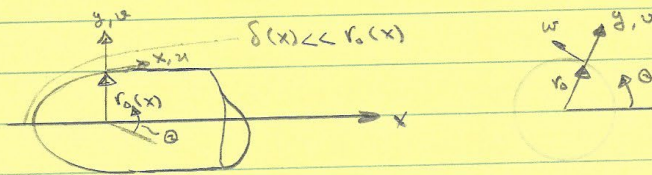
For noncircular sections use D_h & Re_{Dh}

entrance length $\frac{x_L/D}{Re} = 0.08$ ie $K \rightarrow K_{\infty}$ upper bound
 $= 0.01$ where BL meet lower bound
 but BL overlap at too low

$Re_D = 0$
 $x_L/D = 0.6$
 $x_L/D = \frac{0.6}{1 + 0.035 Re_D} + 0.056 Re_D \quad z|_{cl} = 0.99 z_{max}$
 creeping flow so from uniform to parabolic profile fully developed

4.9 Potentially-Symmetric Flow

First, consider the appropriate coordinate system for the 3-d equations for rotationally and axisymmetric flow.



3-d coord: (x, y, θ) with vel components (u, v, w)

The derivation of the rotationally symmetric 3-d equations involves the following steps:

- (1) NS in cylindrical polar coord. (r, θ, x)
- (2) transform to (x, y, θ)
- (3) 3-d approximation
- (4) rotationally symmetric flow assumption $(\frac{\partial}{\partial \theta} = 0)$

$$\frac{\partial}{\partial x}(v_0 u) + v_0 \frac{\partial u}{\partial y} = 0$$

$$\frac{\partial u}{\partial x} + u \frac{\partial u}{\partial x} + v \frac{\partial u}{\partial y} - \frac{\omega^2}{v_0} \frac{dv_0}{dx} = -\frac{1}{\rho} \frac{\partial p}{\partial x} + \nu \frac{\partial^2 u}{\partial y^2}$$

$$0 = \frac{\partial u}{\partial y}$$

$$\frac{\partial u}{\partial x} + u \frac{\partial u}{\partial x} + v \frac{\partial u}{\partial y} + \frac{u v}{v_0} \frac{dv_0}{dx} = \nu \frac{\partial^2 u}{\partial y^2}$$

Outside the vcl, the velocity (U, W) & pressure are related via the Euler equations

$$\frac{\partial U}{\partial z} + U \frac{\partial U}{\partial x} - \frac{W^2}{r_0} \frac{dr_0}{dx} = -\frac{1}{\rho} \frac{\partial p}{\partial x}$$

$$\frac{\partial W}{\partial z} + U \frac{\partial W}{\partial x} + \frac{UW}{r_0} \frac{dr_0}{dx} = 0$$

In general, the bc are

$$y=0: \quad u=0, \quad v = v_w(x, z) \quad w = r_0 \Omega(z)$$

↖ previous wall
↖ velocity body

$$y=\infty: \quad u=U(x, z) \quad w=W(x, z)$$

Some example solutions of the 3d equations for rotationally symmetric flow:

- (1) Rotating flow near a fixed plane
- (2) Rotating sphere
- (3) Conical-swirl atomizer
- (4) Spinning body of revolution
- (5) Decay of a swirling jet (shows interesting result that swirl decays faster than axial velocity)

A considerable amount of work has been done in recent years concerning solutions of higher-order viscous-flow equations (partially parabolic and complete NS) for swirl flows. Some of

The important applications include: combustion flow (swirl is used to promote combustion through swirl-induced mixing & separation); and turbomachinery flow (see display concerning IIR project on propeller-hull interaction)

4.91 Axisymmetric Boundary Layers ($\omega = 0$)

$$\frac{\partial}{\partial x}(v_0 u) + v_0 \frac{\partial v}{\partial y} = 0$$

$$u \frac{\partial u}{\partial x} + v \frac{\partial u}{\partial y} = U \frac{dU}{dx} + v \frac{\partial^2 u}{\partial y^2}$$

$$BC: \quad u(x, 0) = 0 \quad v(x, 0) = v_w(x) \quad u(x, \infty) = U(x)$$

Note: only difference with 2D flow is presence of v_0 in continuity equation

Solution techniques for Axis BL:

- (1) FD
- (2) integral methods
- (3) similarity solution
- (4) Mangler transformation (transformation to equivalent 2D flow)

We shall briefly discuss (2)-(4).

To help motivate the Monger transformation consider the similarity solution for the flow around cones

$U(x) = Cx^n$ potential flow past a cone of half angle α at zero angle of attack $\alpha(n)$ given in Table 4-14
 Similarity transformation is

$$u/U = f'(\eta) \quad \eta = y \left[\frac{(3+n)Cx^{n-1}}{2\nu} \right]^{1/2}$$

$$\Rightarrow f''' + ff'' + \frac{2n}{3+n} (1-f'^2) = 0$$

$$f(0) = f'(0) = 0 \quad f'(\infty) = 1$$

This is equivalent to the Falkner-Skan equation with

$$\beta_{\text{cone}} = \frac{2n}{3+n} = \beta_{\text{wedge}} = \frac{2m}{1+m}$$

ie, $m_{\text{wedge}} = \frac{1}{3} n_{\text{cone}}$

Thus, the cone flow $U = Cx^n$ has similar properties to the wedge flow $U = c'x'^{m/3}$, and the Falkner-Skan equation determines both.

4.92 Monger Transformation

The cone-flow similarity solution suggests the possibility of transforming the AXI 3d equations to an equivalent 2D flow. This was, in fact, accomplished by Monger as follows:

$$\text{let } x' = \frac{1}{L^2} \int_0^x v_0^2 dx \quad y' = v_0 y / L$$

$$u' = u \quad U'(x') = U(x) \quad w' = \frac{L}{v_0} \left(w + \frac{y u}{v_0} \frac{dv_0}{dx} \right)$$

in which L = reference length. With this transformation the AXI 3d equations reduce to

$$\frac{\partial u'}{\partial x'} + \frac{\partial w'}{\partial y'} = 0$$

$$u' \frac{\partial u'}{\partial x'} + w' \frac{\partial u'}{\partial y'} = U' \frac{dU'}{dx'} + \nu \frac{\partial^2 u'}{\partial y'^2}$$

note: (1) All 2D methods discussed previously are applicable

(2) $U'(x')$ does not bear any resemblance to $U(x)$ and may present difficulties in obtaining solutions

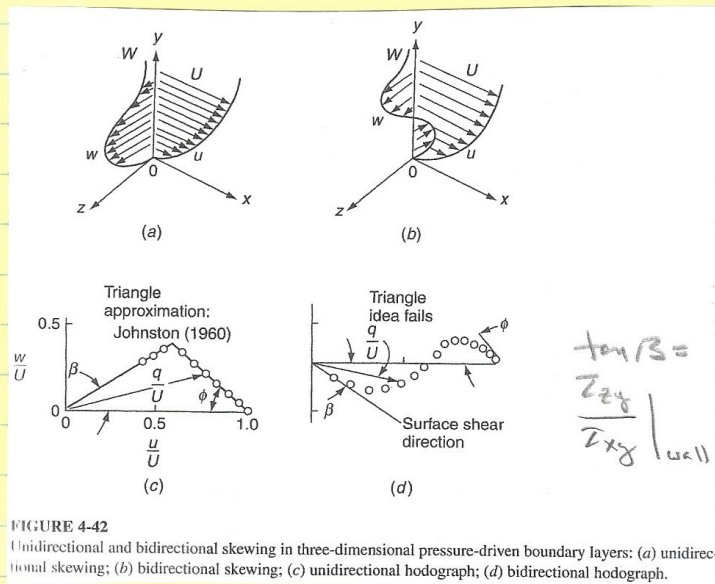
Three dimensional boundary layers

$$u_x + v_y + w_z = 0$$

$$u u_x + v u_y + w u_z = -P_x/\rho + \nu u_{yy}$$

$$u w_x + v w_y + w w_z = -P_z/\rho + \nu w_{yy}$$

Flow driven by
both P_x & P_z



Complex crossflow such as (b): death of 3D
integral methods

Motivated 3D differential BL methods

Thin BL of separation led to rapid
extension differential methods to modern
CFD: RANS, HRLES, LES, DNS!

Boundary layer with constant transverse pressure gradient: flat plate BL with parabolic free stream

Flat plate with LE at $x=0$ & inflow at angle θ_0
 For $x > 0$ & $y \rightarrow \infty$

$$u = u_e = \text{constant} \quad p_x = 0$$

$$w = w_e = u_e (a + bx) \quad -p_z/e = u_e w_{ex} = u_e^2 b$$

External flow $\underline{w} = w_y \hat{j}$ $b = \text{magnitude transverse } p_z$

$$w_y = -\frac{\partial w}{\partial x} = -u_e b$$

For $b=0$ $\theta = \theta_0 = \tan^{-1} \frac{w_e}{u_e} = \tan^{-1} a$, which shows the effect of sweep on Blasius BL

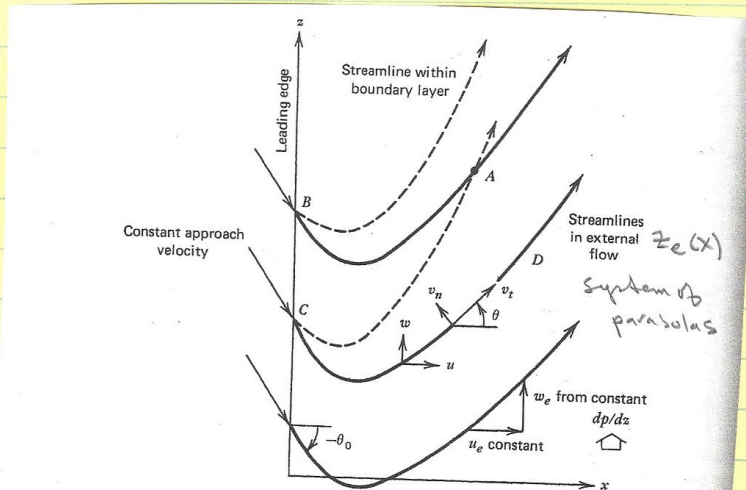


Figure 20.30 Plan view of the boundary layer on a plate with a constant transverse pressure gradient.

$$\frac{dz_e}{dx} = \frac{w_e}{u_e} = a + bx$$

$$z_e = vx + \frac{1}{2}bx^2 + c$$

$$c = \text{constant} = z_e / LE$$

Concept of region of influence: particles that pass through C influence region $\subset A-D$. 3D BL methods must account for spreading influence

BL equations:

$$u_x + v_y = 0$$

$$u u_x + v u_y = \nu u_{yy}$$

$$u v_x + v v_y = \nu v_{yy} + \nu_0^2 + \nu w_{yy}$$

continuity & x-momentum $\neq f(\eta) =$ Blasius BL problem

$$u/u_e = f'(\eta) \quad \eta = y \sqrt{u_e/\nu x}$$

$f(\eta)$ solution Blasius equation: $ff'' + 2f''' = 0$

SwEEP independence principle: u, v solved independent w

$$\text{Assume: } w/u_e = \frac{w_e(x)}{u_e} f'(\eta) + \delta x h(\eta)$$

Blasius component scaled to match $w_e(x)$

Substitution in w -momentum equation

$$h'' + \frac{1}{2} f h' - f' h + 1 - f'^2 = 0$$

$$h(0) = h(\infty) = 0$$

} Similarly Blasius equation solved numerically

Solutions use normal & tangential coordinates to outer flow & normalized with outer flow velocity magnitude $V_\infty = [u_e^2 + w_e^2]^{1/2}$

$$v_t/v_\infty = f'(\gamma) + \frac{1}{2} \sin 2\theta (\tan \theta - \tan \theta_0) h(\gamma)$$

$$v_n/v_\infty = \frac{1}{2} \cos^2 \theta (\tan \theta - \tan \theta_0) h(\gamma)$$

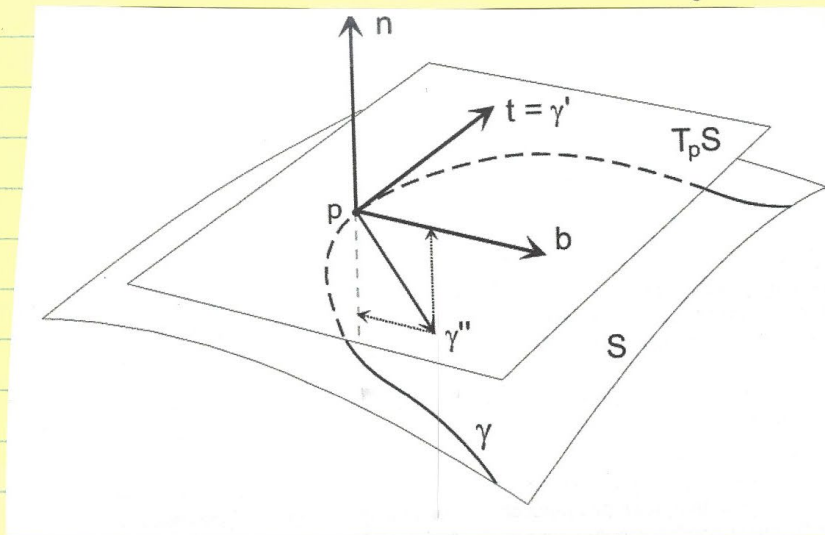
$\theta =$ local inviscid x angle $\tan^{-1} w_c/u_c$

(1) flat plate with sweep angle $\theta = \theta_0$ and $\delta = 0$

Blasius profile of no secondary flow is $v_n = 0$

If γ_c consider with the surface geodesic
 curve $\gamma_{BL} = \gamma_c$ and no secondary flow

Geodesic curve: curve whose tangent vectors
 remain parallel if they are
 transported along it



(2) $\theta \neq 0$ & $b \neq 0$

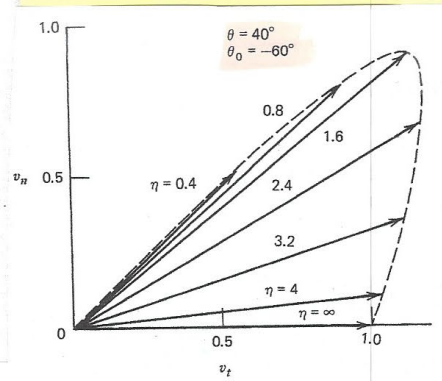
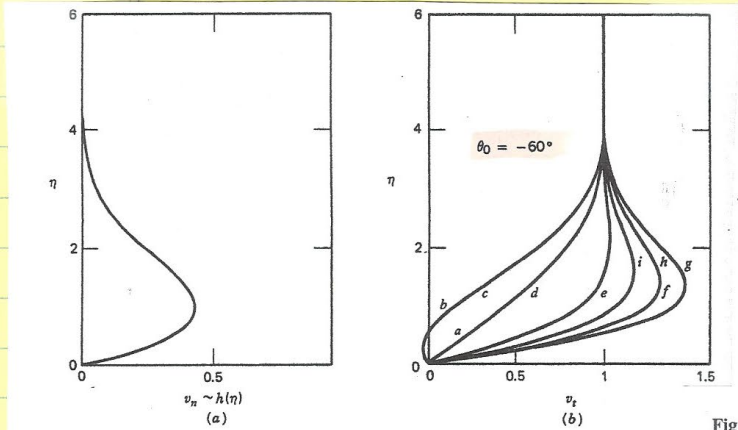


Figure 20.31 Typical velocity profiles: (a) transverse profiles $h(\eta)$; and (b) tangential profiles for various flow angles: a, $\theta = -60^\circ$; b, $\theta = -40^\circ$; c, $\theta = -20^\circ$ (same curve as b); d, $\theta = 0^\circ$ (same as a); e, $\theta = 20^\circ$; f, $\theta = 40^\circ$; g, $\theta = 60^\circ$; h, $\theta = 80^\circ$ (same as f); i, $\theta = 90^\circ$.

Figure 20.32 Polar diagram of velocity profile with overshoot.

θ		v_n not shown since $\propto h(\eta)$
-60	a	Blasius
-40	b	} $v_z < 0$ near $\eta = 0$, but not reverse flow v_n large such that flow > 0 in x direction
-20	c	
0 = a	d	
20	e	} v_z exhibits overshoot in upper BL occurs frequently in 3D BL in thin region (similar as Stokes 2nd problem for oscillating outer flow) net transverse viscous forces some direction pressure force. Viscous force dies out at large η
40	f	
60	g	
80 = f	h	
90	i	

Note: flow never actually separates

$$z_s = \alpha x + \frac{1}{2} \beta x^2 \left[1 + \frac{h'(0)}{f''(0)} \right] + C_0$$
 also parabolic at
 upper zc by $1 + \frac{h'(0)}{f''(0)} \approx 1 + \frac{1}{3}$